Acta Mech 221, 175–200 (2011)
DOI 10.1007/s00707-011-0492-0

Claude-Henri Lamarque · Oleg V. Gendelman · Alireza Ture Savadkoohi · Emilie Etcheverria

Targeted energy transfer in mechanical systems by means of non-smooth nonlinear energy sink

Received: 22 October 2010 / Published online: 7 May 2011

Abstract Targeted energy transfer (TET) in a compound nonlinear 2 degrees-of-freedom system during free and forced excitations is studied analytically and numerically. The nonlinearity of the system is represented intentionally by a non-smooth piece-wise linear function for the sake of practical investigations. Further stability analysis of the system is demonstrated and commented upon and the behavior of the system during relaxation and its strongly modulated response is studied and pinpointed.

1 Introduction

The new generation of nonlinear passive control devices is nonlinear energy sink (NES) devices which can be designed to oscillate with any frequencies and hence can be implemented for the control of broad frequency bands of systems. The theoretical background of these devices is quite extensive [1–14]. There have been some experimental verifications of these devices as well. Readers can refer to [15–23] for detailed information about experimental studies of passive control by NES devices. Most of these studies are based on the cubic nonlinearity of the NES. Nucera et al. [24] and Lee et al. [25] studied the TET in systems with vibro-impact NES, while the TET in a 2 dof system consisting of a linear dof and a nonlinear NES with non-polynomial and piece-wise potential is investigated by Gendelman [26]. In this paper, we did a detailed investigation on a 2 dof system with a non-smooth NES under free and forced vibrations. The organization of the article is as it follows: The general description of the system under consideration is illustrated in Sect. 2. The mentioned system under impulse loadings is pinpointed in Sect. 3. The behavior of the system in the form of amplitudes of two oscillators, effective system parameters on this behavior, further stability analysis, and finally the comparison between analytical and numerical results are carried out in the same section. The system under external solicitations is studied in Sect. 4. The behavior of the system during the TET and stability analysis are discussed in the same section. SMR of the system and necessary conditions for the relaxation are investigated in Sect. 5. Finally, conclusions are gathered in Sect. 6.

C.-H. Lamarque · A. Ture Savadkoohi (✉) · E. Etcheverria
Université de Lyon, École Nationale des Travaux Publics de l'État, DGCB, FRE CNRS 3237,
3 rue Maurice Audin, 69518 Vaulx-en-Velin Cedex, France
E-mail: alireza.turesavadkoohi@entpe.fr
Tel.: +33 (0) 4 72 04 70 75
Fax.: +33 (0) 4 72 04 71 56

O. V. Gendelman
Faculty of Mechanical Engineering, Technion-Israel Institute of Technology, 32000 Technion City, Haifa, Israel

2 The general description of the system

Let us consider following mathematical model of the system under consideration [26] which represents a 2 dof system involving a linear master dof and a non-smooth NES. The mass of the NES is considered to be very small compared with the mass of the master structure. ϵ is the mass ratio between the NES and the master dof, respectively, so $\epsilon \ll 1$.

$$\begin{cases} \ddot{y}_1 + \epsilon\lambda(\dot{y}_1 - \dot{y}_2) + y_1 + \epsilon F(y_1 - y_2) = \epsilon f_0 \sin(\omega t), \\ \epsilon\ddot{y}_2 + \epsilon\lambda(\dot{y}_2 - \dot{y}_1) + \epsilon F(y_2 - y_1) = 0, \end{cases} \tag{1}$$

where the non-smooth potential function $F(z)$ is defined as

$$F(z) = \begin{cases} 0 & \text{if } -a \le z \le a, \\ c(z-a) & \text{if } z \ge a, \\ c(z+a) & \text{if } z \le -a. \end{cases} \tag{2}$$

We study the system (1) in the vicinity of the 1:1 resonance. Let us introduce coordinates of the center of mass and the relative displacement of the 2 dof system:

$$\begin{cases} v = y_1 + \epsilon y_2, \\ w = y_1 - y_2, \end{cases} \tag{3}$$

then the system in the new coordinates takes the form

$$\begin{cases} \ddot{v} + \frac{1}{1+\epsilon}(v + \epsilon w) = \epsilon f_0 \sin(\omega t), \\ \\ \ddot{w} + \frac{1}{1+\epsilon}(v + \epsilon w) + (1+\epsilon)\lambda\dot{w} + (1+\epsilon)F(w) = \epsilon f_0 \sin(\omega t). \end{cases} \tag{4}$$

3 The system under free oscillation

Let us consider the system when $f_0 = 0$. We introduce complex variables of Manevitch as follows [27]:

$$\begin{cases} \varphi_1 e^{it} = \dot{v} + iv, \\ \varphi_2 e^{it} = \dot{w} + iw, \end{cases} \tag{5}$$

where $i = \sqrt{-1}$. We can present the function $F(w)$ in the form of a Fourier series [26]:

$$F(w) = F\left(-\frac{i}{2}(\varphi_2 e^{it} - \varphi_2^* e^{-it})\right) = \sum_{j=-\infty}^{+\infty} f_j(\varphi_2, \varphi_2^*) e^{ijt}, \tag{6}$$

where the $.^*$ represents the complex conjugate of the function under consideration. The above-mentioned variables and assumptions lead the averaged system (4) to

$$\begin{cases} \dot{\varphi}_1 + \frac{i\epsilon}{2(1+\epsilon)}(\varphi_1 - \varphi_2) = 0, \\ \dot{\varphi}_2 + \frac{i}{2(1+\epsilon)}(\varphi_2 - \varphi_1) + \frac{\lambda(1+\epsilon)}{2}\varphi_2 + (1+\epsilon) f_1(\varphi_2, \varphi_2^*) = 0, \end{cases} \tag{7}$$

where $f_1(\varphi_2, \varphi_2^*)$ is the first Fourier coefficient:

$$f_1(\varphi_2, \varphi_2^*) = \frac{1}{2\pi}\int_0^{2\pi} F\left(-\frac{i}{2}(\varphi_2 e^{it} - \varphi_2^* e^{-it})\right) e^{-it}\, \mathrm{d}t. \tag{8}$$

It is proved by Gendelman [26] that

$$f_1(\varphi_2, \varphi_2^*) = -\frac{i\varphi_2}{2} G\left(|\varphi_2|^2\right), \tag{9}$$

where

$$G\left(|\varphi_2|^2\right) = \begin{cases} 0 & \text{if } |\varphi_2| < a, \\ \frac{1}{\pi}\left(2c\arccos\left(\frac{a}{|\varphi_2|}\right) - \frac{2ac\sqrt{|\varphi_2|^2-a^2}}{|\varphi_2|^2}\right) & \text{if } |\varphi_2| \geq a. \end{cases} \tag{10}$$

To deal with the averaged system of (7), an asymptotic approach [28] by introducing slow times $\tau_1, \tau_2, \ldots$ with the fast time τ_0 can be implemented as follows:

$$t = \tau_0, \qquad \tau_1 = \epsilon\tau_0, \ \ldots, \tag{11}$$

so

$$\frac{\partial}{\partial\tau_0} + \epsilon\frac{\partial}{\partial\tau_1} + \cdots := \frac{\mathrm{d}}{\mathrm{d}t}. \tag{12}$$

The system of equations (7) is now examined for different orders of ϵ.

3.1 Order ϵ^0

For order of ϵ^0, the expansion (12) yields:

$$\begin{cases} \frac{\partial\varphi_1}{\partial\tau_0} = 0 \Rightarrow \varphi_1 = \varphi_1(\tau_1), \\ \frac{\partial\varphi_2}{\partial\tau_0} + \frac{i\left(1-G\left(|\varphi_2|^2\right)\right)+\lambda}{2}\varphi_2 = \frac{i}{2}\varphi_1. \end{cases} \tag{13}$$

Fixed points $\Phi(\tau_1)$ of the system (13) are evaluated as

$$\frac{i\left(1-G\left(|\Phi|^2\right)\right)+\lambda}{2}\Phi = \frac{i}{2}\varphi_1. \tag{14}$$

Let us assume that $\varphi_1 = N_1 e^{i\delta_1}$ and $\Phi = N_2 e^{i\delta_2}$, so Eq. (14) can be re-written in the following form:

$$N_2 - i\lambda N_2 - G\left(N_2^2\right)N_2 = N_1 e^{i(\delta_1-\delta_2)}. \tag{15}$$

By separating real and imaginary parts of Eq. (15), one can reach the following system:

$$\begin{cases} N_2\left(1-G\left(N_2^2\right)\right) = N_1\cos(\delta_2-\delta_1), \\ \lambda N_2 = N_1\sin(\delta_2-\delta_1), \end{cases} \tag{16}$$

so

$$N_1 = N_2\sqrt{\lambda^2 + \left(1-G\left(N_2^2\right)\right)^2}. \tag{17}$$

Depending on the combination of system parameters, there will be one, two, or three fixed points. The variation of N_1 with respect to N_2 for some chosen system parameters is illustrated in Fig. 1. This figure shows that for given system parameters and depending on the initial value of N_1, the system can have one, two, or three fixed points. Local extrema of Eq. (17) can be revealed by the criterium

$$\frac{\partial N_1^2}{\partial N_2^2} = 0, \tag{18}$$

which finally yields the equation

$$1 + \lambda^2 + G^2\left(N_2^2\right) - 2G\left(N_2^2\right) - 2N_2^2G'\left(N_2^2\right) + 2N_2^2G'\left(N_2^2\right)G\left(N_2^2\right) = 0. \tag{19}$$

Equation (19) can not be verified for $N_2 < a$, so local extrema associated to (19) have to be traced for $N_2 \geq a$. Let us assume that

$$Y = 2\arccos\left(\frac{a}{N_2}\right), \tag{20}$$

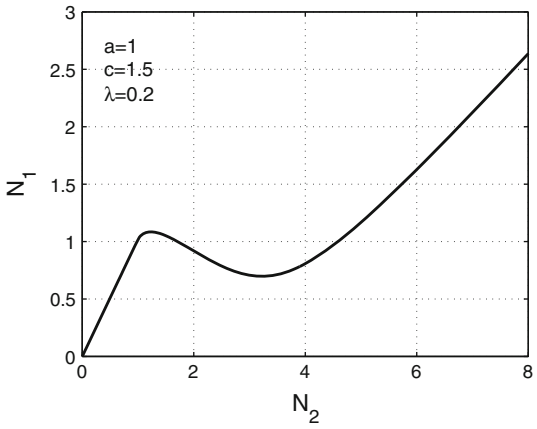

Fig. 1 N_1 vs. N_2 for the system under free vibration

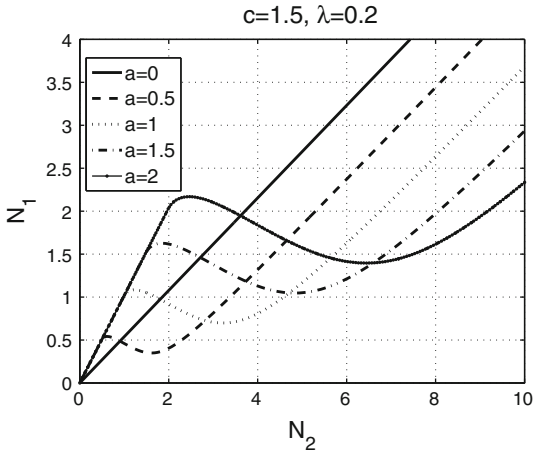

Fig. 2 N_1 vs. N_2 for varying parameter a

so

$$\sin^2(Y) = \left(\frac{\lambda\pi}{c}\right)^2 + \left(Y - \frac{\pi}{c}\right)^2. \tag{21}$$

This equation does not depend on the parameter a and gives two solutions for Y ($Y_i, i = 1, 2$); so the position of the extreme $N_{2,i}, i = 1, 2$ can be evaluated by endowing Eq. (20) as follows:

$$N_{2,i} = \frac{a}{\cos\left(\frac{Y_i}{2}\right)}, \tag{22}$$

$$N_{1,i} = \frac{a}{\cos\left(\frac{Y_i}{2}\right)}\sqrt{\lambda^2 + \left(1 - \frac{c\,(Y_i - \sin(Y_i))}{\pi}\right)^2}. \tag{23}$$

Extreme values are proportional to value of the parameter a. Figure 2 summarizes effects of the parameter a on the position of the extrema. The sensitivity of the system to the parameter c is illustrated in Fig. 3 which shows that for $c \leq 1$ the system does not have any extremum. This fact can be clarified by examining Eq. (21) which shows that the function $f(Y) = \left(\frac{\lambda\pi}{c}\right)^2 + \left(Y - \frac{\pi}{c}\right)^2 - \sin^2(Y)$, $Y \in [0, \pi]$ does not have any extremum for $c \leq 1$. Finally, variation of N_1 versus N_2 with respect to λ is depicted in Fig. 4. For $\lambda > 0.4$, there is no extremum. This critical value of damping for the given system can be understood and explained by examining the above-mentioned function. Moreover, it can be seen that for a system without damping the local minimum is zero.

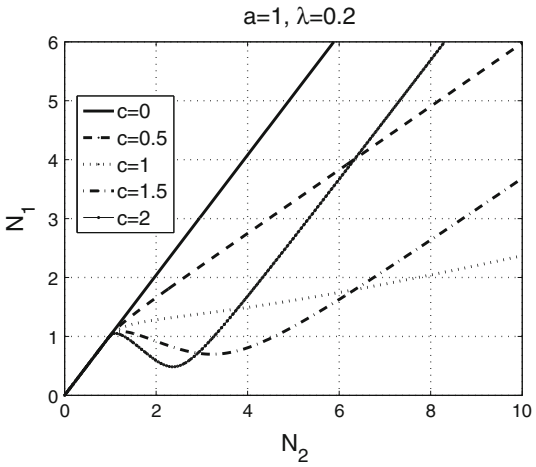

Fig. 3 N_1 vs. N_2 for varying parameter c

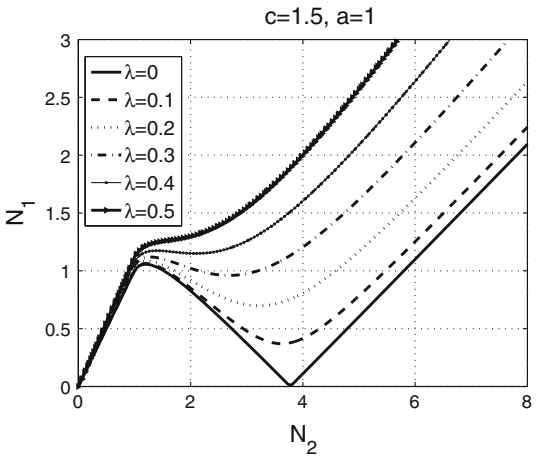

Fig. 4 N_1 vs. N_2 for varying parameter λ

3.1.1 Stability analysis

Let us assume following perturbation:

$$\begin{cases} N_1 \to N_1 + \triangle N_1, \\ \delta_1 \to \delta_1 + \triangle \delta_1, \\ N_2 \to N_2 + \triangle N_2, \\ \delta_2 \to \delta_2 + \triangle \delta_2. \end{cases} \tag{24}$$

We linearize the system (16) around its fixed points. We obtain:

$$G\left(\left(N_2 + \triangle N_2\right)^2\right) = G\left(N_2^2\right) + H\left(N_2^2\right)\triangle N_2, \tag{25}$$

$$H\left(N_2^2\right) = \begin{cases} 0, N_2 < a, \\ \frac{4ac}{\pi N_2^3}\sqrt{N_2^2 - a^2}, N_2 \geq a. \end{cases} \tag{26}$$

After some mathematical manipulations, the linearized form of the above-mentioned system reads

$$\begin{bmatrix} \frac{\partial(\triangle N_1)}{\partial \tau_0} \\ \frac{\partial(\triangle \delta_1)}{\partial \tau_0} \\ \frac{\partial(\triangle N_2)}{\partial \tau_0} \\ \frac{\partial(\triangle \delta_2)}{\partial \tau_0} \end{bmatrix} = M \begin{bmatrix} \triangle N_1 \\ \triangle \delta_1 \\ \triangle N_2 \\ \triangle \delta_2 \end{bmatrix}, \tag{27}$$

where

$$M = \begin{bmatrix} 0 & 0 & 0 & 0 \\ 0 & 0 & 0 & 0 \\ M_{31} & M_{32} & -\frac{\lambda}{2} & M_{34} \\ M_{41} & \frac{\lambda}{2} & M_{43} & -\frac{\lambda}{2} \end{bmatrix} \tag{28}$$

and

$$\begin{cases} M_{31} = \frac{\lambda N_2}{2N_1}, \\ M_{32} = -\frac{1}{2} N_2 \left(1 - G\left(N_2^2\right)\right), \\ M_{34} = \frac{1}{2} N_2 \left(1 - G\left(N_2^2\right)\right), \\ M_{41} = \frac{1}{2N_1} \left(1 - G\left(N_2^2\right)\right), \\ M_{43} = -\frac{1}{2N_2} \left(1 - G\left(N_2^2\right)\right) + \frac{1}{2} H\left(N_2^2\right). \end{cases} \tag{29}$$

The characteristic equation of the matrix M is:

$$P(X) = X^2 \left(X^2 + \lambda X + \frac{\lambda^2}{4} - M_{34} M_{43} \right). \tag{30}$$

Two eigenvalues of the system are always zero. The sum of the eigenvalues is $-\lambda < 0$ and their product is $\frac{\lambda^2}{4} - M_{34} M_{43}$. In order to pinpoint the system from a stability view point, we consider the following cases:

- $\frac{\lambda^2}{4} - M_{34} M_{43} < 0$

  Two eigenvalues are real with opposite signs. The fixed point is unstable.
- $\frac{\lambda^2}{4} - M_{34} M_{43} > 0$

  Two eigenvalues can be complex or real. If they are complex, then they will have the same real part equal to $-\frac{\lambda}{2} < 0$; so the fixed points are stable. If the eigenvalues are real, then they will be negative; again the fixed points will be stable.
- $\frac{\lambda^2}{4} - M_{34} M_{43} = 0$

  One of the eigenvalues is zero and the other one is $-\lambda < 0$. The fixed point is stable.

As a summary, the necessary condition for the stability can be studied by following criteria:

$$\frac{\lambda^2}{4} - M_{34} M_{43} \geq 0 \Longleftrightarrow \lambda^2 + \left(1 - G\left(N_2^2\right)\right)\left(1 - H\left(N_2^2\right) N_2 - G\left(N_2^2\right)\right) \geq 0. \tag{31}$$

By endowing introduced variables of (20), the condition of (31) is equivalent to

$$\left(\frac{\lambda \pi}{c}\right)^2 + \left(Y - \frac{\pi}{c}\right)^2 - \sin^2 Y \geq 0, \tag{32}$$

so we can distinguish two different cases:

- $c \leq 1$

  All fixed points are stable.

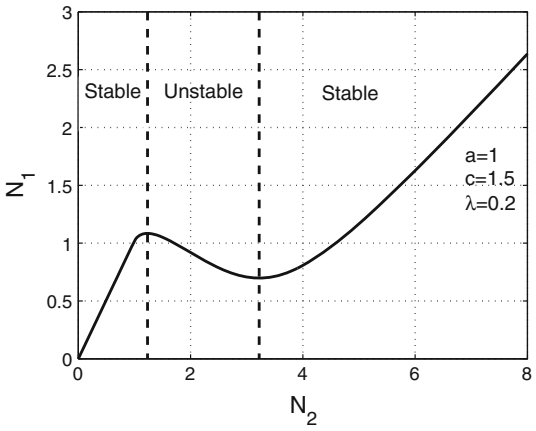

Fig. 5 Stable and unstable zones of fixed points

– $c > 1$
Let us suppose that λ_c is the critical damping which defines the maximum damping value for the system in order to have extrema: if $\lambda \geq \lambda_c$ then all fixed points are stable. If $\lambda < \lambda_c$, then fixed points staying between two extrema (i.e. $N_{21} < N_2 < N_{22}$) are unstable.

Typical stable and unstable zones of fixed points for given system parameters are depicted in Fig. 5.

3.2 Order ϵ^1

Let us pinpoint the system (7) around the order ϵ^1 of the perturbed equations. The first equation of the mentioned system reads

$$\frac{\partial \varphi_1}{\partial \tau_1} + \frac{i}{2}(\varphi_1 - \Phi) = 0. \tag{33}$$

By replacing the φ_1 from (14) in Eq. (33), the following system can be derived:

$$\frac{\partial}{\partial \tau_1}\left(\Phi - i\lambda\Phi - \Phi G\left(|\Phi|^2\right)\right) + \frac{\lambda}{2}\phi - \frac{i}{2}\Phi G(|\Phi|^2) = 0. \tag{34}$$

By separating the real and imaginary parts of Eq. (34), one can reach the following system:

$$\frac{\partial N_2}{\partial \tau_1} = \frac{-\lambda N_2}{2\left(1 + \lambda^2 + G^2\left(N_2^2\right) - 2G\left(N_2^2\right) - 2N_2^2 G'\left(N_2^2\right) + 2N_2^2 G\left(N_2^2\right) G'\left(N_2^2\right)\right)}, \tag{35}$$

$$\frac{\partial \delta_2}{\partial \tau_1} = \frac{-\lambda^2 + G\left(N_2^2\right) - G^2\left(N_2^2\right) - 2N_2^2 G'\left(N_2^2\right)}{2\left(1 + \lambda^2 + G^2\left(N_2^2\right) - 2G\left(N_2^2\right) - 2N_2^2 G'\left(N_2^2\right) + 2N_2^2 G\left(N_2^2\right) G'\left(N_2^2\right)\right)}. \tag{36}$$

Let us study the zeros of the denominator of Eqs. (35) and (36).

$$2\left(1 + \lambda^2 + G^2\left(N_2^2\right) - 2G\left(N_2^2\right) - 2N_2^2 G'\left(N_2^2\right) + 2N_2^2 G\left(N_2^2\right) G'\left(N_2^2\right)\right) = 0. \tag{37}$$

Equation (37) does not have any solution when $c \leq 1$, so the system (35) and (36) will not be singular. If $c > 1$, two scenarios are possible for the behavior of the system:

If $\lambda \geq \lambda_c$, then Eq. (37) will not have any solution, the system will not be singular and Eq. (35) will not change its sign and it will always be negative.

If $\lambda < \lambda_c$, then Eq. (37) will have two solutions and there will be a sudden drop and jump in the $N_1 - N_2$ diagram.

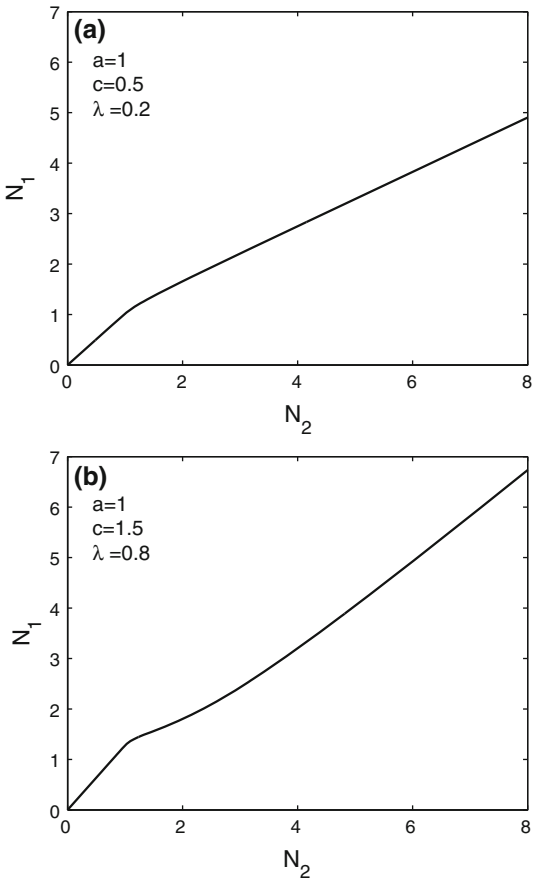

Fig. 6 The system without TET: **a** $c < 1$; **b** $c > 1$ and $\lambda \geq \lambda_c$

3.3 Description of the phenomenon

Let us consider different possibilities of the system under consideration:

3.3.1 $c < 1$ or $\lambda \geq \lambda_c$

The equation (17) does not have any extremum, all fixed points of the system are stable and Eqs. (35) and (36) are not singular. The energy of the system decreases continuously without any sharp drop. This is a classic case of control without any evidence of the TET which is summarized in Fig. 6.

3.3.2 $c \geq 1$ or $\lambda < \lambda_c$

The equation (17) has two extrema where Eqs. (35) and (36) are singular. Let us suppose that $N_{1\text{act}}$ is the local maximum of the system; according to the initial energy two scenarios are possible:

If $N_1 < N_{1\text{act}}$, then systems (35) and (36) would not face singularities and the energy of the system decreases continually and smoothly. As a results, the system will not experience the TET. Figure 7 schematically illustrates a typical system without sufficient activation energy for the TET.

If $N_1 \geq N_{1\text{act}}$, then energy of the system will decrease continually until it reaches to the singularity points of systems (35) and (36). Then the system will face an abrupt decrease in energy, which indicates the evidence of the TET (see Fig. 8).

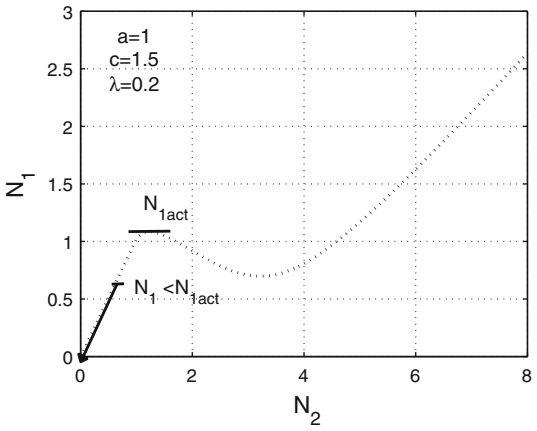

Fig. 7 Insufficient initial energy for the TET

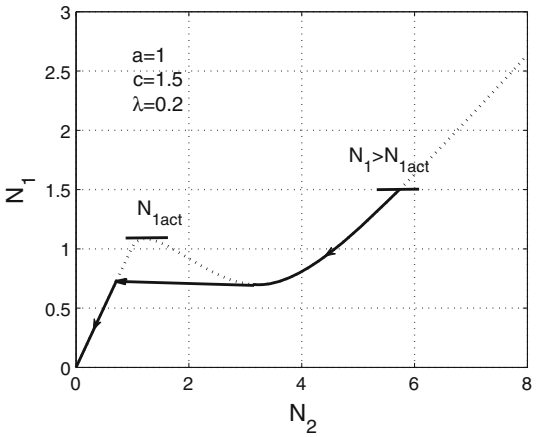

Fig. 8 Sufficient initial energy for the TET

3.4 Numerical verifications

By considering the definition of φ_1 and φ_2, N_1 and N_2 can be defined in terms of original system of equations (N_1^{exact} and N_2^{exact}) as follows:

$$N_1^{\text{exact}} = \sqrt{(y_1 + \epsilon y_2)^2 + (\dot{y_1} + \epsilon \dot{y_2})^2}, \tag{38}$$

$$N_2^{\text{exact}} = \sqrt{(y_1 - y_2)^2 + (\dot{y_1} - \dot{y_2})^2}, \tag{39}$$

where y_1 and y_2 can be evaluated by direct integration of the system (1); moreover, we suppose following initial conditions for the system:

$$\begin{cases} y_1(0) = 4, & \dot{y}_1(0) = 0, \\ y_2(0) = 0, & \dot{y}_2(0) = 0. \end{cases} \tag{40}$$

Numerical results obtained by integration of the system (1) by the "rk45" function of Matlab and corresponding analytical ones which are revealed from the averaged system (7) in terms of N_1 and N_2 are illustrated in Figs. 9 and 10, respectively. These figures show that N_2 increases rapidly until $t = 25$ s, which means that the energy of the master system is transferred to the non-smooth auxiliary oscillator and then there is an abrupt decrease in N_2 due to the singularity and sudden jump. Moreover, these figures give a hint about the good agreement between numerical and analytical results until just after the sudden jump of the system. After this moment, numerical and analytical results of the N_2 do not match well. This can be due to the $1:1$ resonance that is not valid any more. But it is not important since the control has been performed.

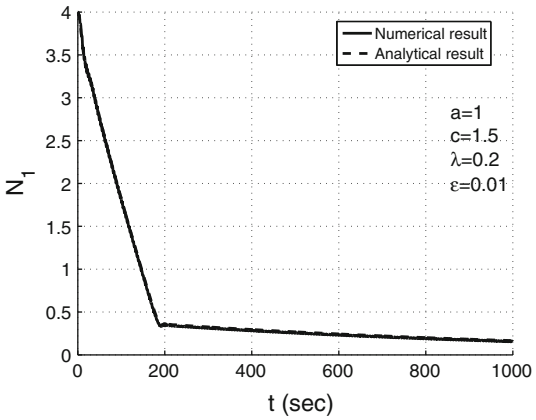

Fig. 9 Numerical and analytical results for N_1 during the free vibration

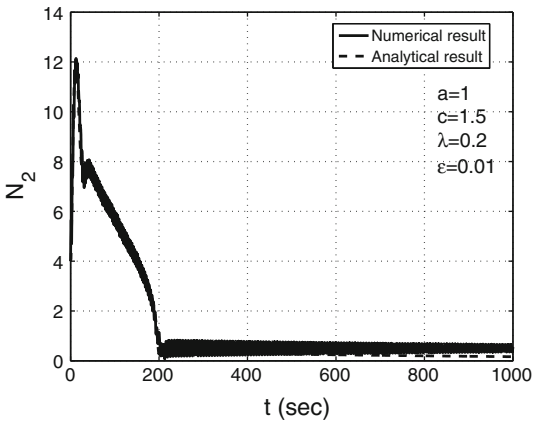

Fig. 10 Numerical and analytical results for N_2 during free vibration

Let us suppose following initial conditions of the system:

$$\begin{cases} y_1(0) = 1.5, & \dot{y}_1(0) = 0, \\ y_2(0) = 0, & \dot{y}_2(0) = 0. \end{cases} \tag{41}$$

The responses of the system in terms of N_1 versus N_2 that are obtained from numerical integration for two different ϵ parameters and analytically obtained from Eq. (17) are depicted in Fig. 11. Since the initial energy is greater than the activation energy $N_{1\text{act}}$, and the damping is less than the critical damping, the system experiences the TET. There are some differences between numerical and analytical results in Fig. 11a. These differences are due to the parameter ϵ. In fact, smaller ϵ provides more precise numerical results (see Fig. 11b). This figure shows the efficiency of NES devices with non-smooth nonlinearities in controlling the main system under impulse loadings provided that the initial energy is large enough to activate the NES. Figure 12 shows histories of displacements of the master system and non-smooth NES versus time with the initial conditions (41). One can observe that the displacement of the main oscillator decreases rapidly while a large part of the energy is transferred to the attached non-smooth oscillator which exhibits strong oscillations.

4 Forced system

Here, we examine the behavior of the system (1) when $f_0 \neq 0$. Moreover, we suppose that $\omega = 1 + \sigma\epsilon$. In this case, the complex variables of Manevitch take the following form [27]:

$$\begin{cases} \varphi_1 e^{i\omega t} = \dot{v} + i\omega v, \\ \varphi_2 e^{i\omega t} = \dot{w} + i\omega w, \end{cases} \tag{42}$$

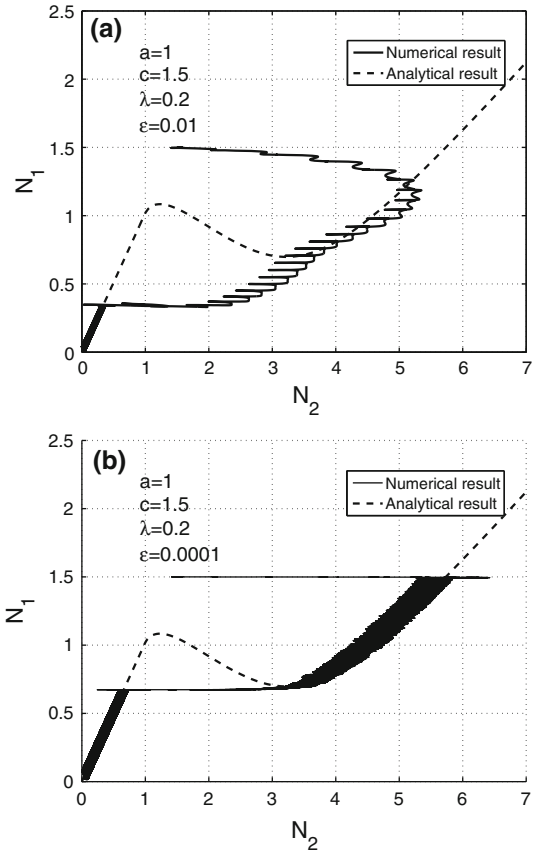

Fig. 11 Numerical and analytical results for N_1-N_2: **a** $\epsilon = 0.01$; **b** $\epsilon = 0.0001$

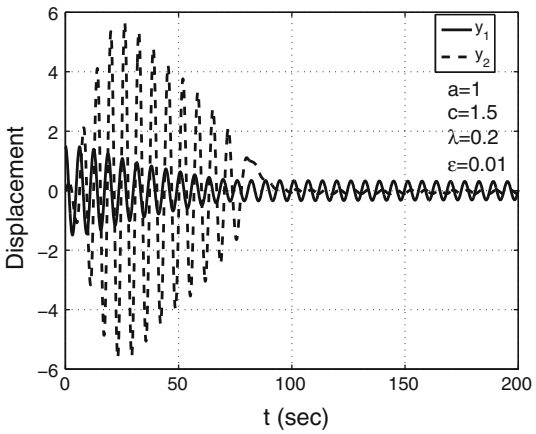

Fig. 12 Displacement histories of two oscillators

so the functions $F(w)$ and $f_1(\varphi_2, \varphi_2^*)$ read:

$$F(w) = F\left(-\frac{i}{2\omega}\left(\varphi_2 e^{i\omega t} - \varphi_2^* e^{-i\omega t}\right)\right) = \sum_{j=-\infty}^{+\infty} f_j\left(\varphi_2, \varphi_2^*\right) e^{i\omega j t}, \tag{43}$$

$$f_1(\varphi_2, \varphi_2^*) = \frac{\omega}{2\pi} \int_0^{2\pi} F\left(-\frac{i}{2\omega}\left(\varphi_2 e^{i\omega t} - \varphi_2^* e^{-i\omega t}\right)\right) e^{-i\omega t}\, \mathrm{d}t, \tag{44}$$

or

$$f_1\left(\varphi_2, \varphi_2^*\right) = -\frac{i\varphi_2}{2} G\left(|\varphi_2|^2\right), \tag{45}$$

and the function $G\left(|\varphi_2|^2\right)$ is governed by Eq. (10). Considering all above mentioned definitions in the system (4), one can reach the following averaged system of equations:

$$\begin{cases} \dot{\varphi}_1 = -\frac{i}{2}\epsilon f_0 + \frac{i}{2\omega(1+\epsilon)}(\varphi_1 + \epsilon\varphi_2) - \frac{i}{2}\omega\varphi_1, \\ \dot{\varphi}_2 = -\frac{i}{2}\epsilon f_0 + \frac{i}{2\omega(1+\epsilon)}(\varphi_1 + \epsilon\varphi_2) - \frac{\lambda(1+\epsilon)}{2}\varphi_2 - \frac{i}{2}\omega\varphi_2 \\ \qquad + \frac{i(1+\epsilon)}{2} G\left(|\varphi_2|^2\right)\varphi_2. \end{cases} \tag{46}$$

After introducing slow and fast time scales as in Eq. (11) and using multiple scale analysis technique [28], different orders of ϵ should be considered.

4.1 Order ϵ^0

The system (46) at the order ϵ^0 yields:

$$\frac{\partial\varphi_1}{\partial\tau_0} = 0 \Rightarrow \varphi_1 = \varphi_1(\tau_1), \tag{47}$$

$$\frac{\partial\varphi_2}{\partial\tau_0} + \frac{i\left(1 - G\left(|\varphi_2|^2\right)\right) + \lambda}{2}\varphi_2 = \frac{i}{2}\varphi_1, \tag{48}$$

so, fixed points of the system can be evaluated by the following equation:

$$\frac{i\left(1 - G\left(|\phi|^2\right)\right) + \lambda}{2}\Phi = \frac{i}{2}\varphi_1, \tag{49}$$

which is exactly Eq. (14); i.e., fixed points for the system under free and forced oscillations are the same. So, we will have the same relationship between N_1 and N_2 as is illustrated in Eq. (17).

4.2 Order ϵ^1

At the order ϵ^1, the first equation of the system (46) reads:

$$\frac{\partial\varphi_1}{\partial\tau_1} = -\frac{i}{2}f_0 - \frac{i}{2}((2\sigma + 1)\varphi_1 - \Phi). \tag{50}$$

By replacing the φ_1 from Eq. (49) in the system (50), one can obtain

$$\begin{aligned} &\frac{\partial}{\partial\tau_1}\left(\Phi - i\lambda\Phi - G\left(|\Phi_2|^2\right)\Phi\right) \\ &= -\frac{i}{2}\left(-f_0 - 2\sigma\left(\Phi - i\lambda\Phi - G\left(|\Phi|^2\right)\Phi\right) + i\lambda\Phi + G\left(|\Phi|^2\right)\Phi\right). \end{aligned} \tag{51}$$

Let us consider that in the Eq. (51), $\Phi = N_2(\tau_1)e^{i\delta_2(\tau_1)}$; by separating real and imaginary parts of the obtained system, following compact form of the equations comes out:

$$\frac{\partial N_2}{\partial\tau_1} = \frac{f_1(N_2, \delta_2)}{g(N_2)}, \tag{52}$$

$$\frac{\partial\delta_2}{\partial\tau_1} = \frac{f_2(N_2, \delta_2)}{g(N_2)}, \tag{53}$$

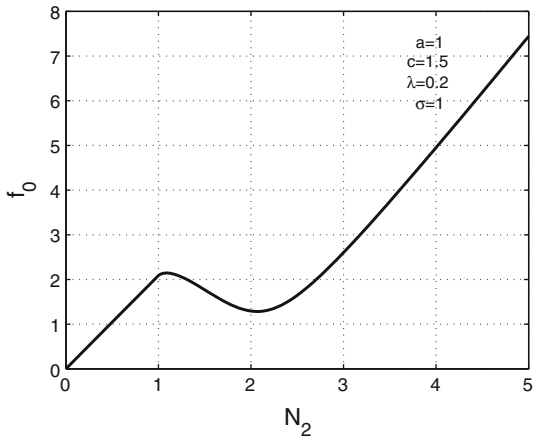

Fig. 13 f_0 versus N_2

where

$$f_1(N_2,\delta_2) = f_0\sin(\delta_2)\left(G\left(N_2^2\right)-1\right)-\lambda N_2+\lambda f_0\cos(\delta_2), \tag{54}$$

$$f_2(N_2,\delta_2) = -\frac{1-G\left(N_2^2\right)-2N_2^2G'\left(N_2^2\right)}{N_2}f_0\cos(\delta_2)-\frac{\lambda}{N_2}f_0\sin(\delta_2)$$
$$-\lambda^2(1+2\sigma)+\left(1-G\left(N_2^2\right)-2N_2^2G'\left(N_2^2\right)\right)\left(-2\sigma+2\sigma G\left(N_2^2\right)+G\left(N_2^2\right)\right), \tag{55}$$

$$g(N_2) = 2\left(1+\lambda^2-2G\left(N_2^2\right)-2N_2^2G'\left(N_2^2\right)+G^2\left(N_2^2\right)+2N_2^2G\left(N_2^2\right)G'\left(N_2^2\right)\right). \tag{56}$$

Since $g(N_2)$ is the same as the denominators of Eqs. (35) and (36), all singular points and necessary conditions for pumping in the free and forced vibration cases are the same.
Let us study the behavior of the system during its steady-state regime. From Eq. (51), we have:

$$\frac{i}{2}\left(-f_0-2\sigma\left(\Phi-i\lambda\Phi-G\left(|\Phi|^2\right)\Phi\right)+i\lambda\Phi+G\left(|\Phi|^2\right)\Phi\right)=0 \tag{57}$$

so

$$f_0 = N_2\sqrt{\lambda^2(1+2\sigma)^2+\left((1+2\sigma)G\left(N_2^2\right)-2\sigma\right)^2}. \tag{58}$$

For given parameters, a typical diagram of f_0 versus N_2 is illustrated in Fig. 13.
Local extrema of the function f_0 in Eq. (58) can be revealed by imposing the following criterion:

$$\frac{\partial f_0^2}{\partial N_2^2}=0, \tag{59}$$

so

$$2N_2\left(\lambda^2(1+2\sigma)^2+\left((1+2\sigma)G\left(N_2^2\right)-2\sigma\right)^2\right)$$
$$+4N_2^2(1+2\sigma)G'\left(N_2^2\right)\left((1+2\sigma)G\left(N_2^2\right)-2\sigma\right)=0 \qquad N_2\geq a. \tag{60}$$

Let us introduce the variable Y of Eq. (20) in the system (60); this yields:

$$\sin^2(Y) = \left(\frac{\lambda\pi}{c}\right)^2+\left(Y-\frac{2\sigma\pi}{c(2\sigma+1)}\right)^2. \tag{61}$$

As in the case of the system under free vibration, this function can be studied in the interval $[0,\pi]$. If $\frac{2\sigma}{c(2\sigma+1)}\leq 0$ or $\frac{2\sigma}{c(2\sigma+1)}\geq 1$ then the function f_0 doesn't have any extreme. If $0<\frac{2\sigma}{c(2\sigma+1)}<1$, then according to c and λ parameters, the system will have no or two extrema.

4.3 Stability analysis

Let us perturb N_2 and δ_2 as in Eq. (24). If we define following parameters:

$$\begin{cases} A = 1 - G\left(N_2^2\right) - H\left(N_2^2\right) N_2, \\ B = -\lambda(2\sigma + 1), \\ C = -(2\sigma + 1)G\left(N_2^2\right) + 2\sigma, \\ D = G\left(N_2^2\right) + H\left(N_2^2\right) N_2, \\ \Delta = \left(A\left(1 - G\left(N_2^2\right) + \lambda^2\right) N_2, \end{cases} \tag{62}$$

and $H\left(N_2^2\right)$ given by (26), then after some mathematical manipulations the linearized form of the system around its fixed points reads:

$$\begin{bmatrix} \frac{\partial N_2}{\partial \tau_1} \\ \\ \frac{\partial \delta_2}{\partial \tau_1} \end{bmatrix} = \frac{1}{\Delta} M \begin{bmatrix} \triangle N_2 \\ \triangle \delta_2 \end{bmatrix}, \tag{63}$$

where

$$M = \begin{bmatrix} M_{11} & M_{12} \\ M_{21} & M_{22} \end{bmatrix} \tag{64}$$

and

$$\begin{cases} M_{11} = \left(\frac{B}{2}\left(1 - G\left(N_2^2\right)\right) + \frac{\lambda}{2}\left(D - 2\sigma A\right)\right) N_2, \\ M_{12} = \left(\frac{C}{2}\left(1 - G\left(N_2^2\right)\right) - \frac{\lambda B}{2}\right) N_2^2, \\ M_{21} = \frac{A}{2}(D - 2\sigma A) + \frac{\lambda B}{2}, \\ M_{22} = \left(\frac{AB}{2} + \frac{\lambda C}{2}\right) N_2. \end{cases} \tag{65}$$

Necessary conditions for the stability of the system around its fixed points can be summarized as

$$\left(\frac{\lambda\pi}{c}\right)^2 + \left(Y - \frac{2\sigma\pi}{c(2\sigma + 1)}\right)^2 - \sin^2(Y) \geq 0. \tag{66}$$

Now, we can distinguish two different cases:

– $\dfrac{2\sigma}{c(2\sigma + 1)} \leq 0$ or $\dfrac{2\sigma}{c(2\sigma + 1)} \geq 1$.

All fixed points are stable.

– $0 < \dfrac{2\sigma}{c(2\sigma + 1)} < 1$.

Let us suppose that λ_c is the critical damping which defines the border between existence of extrema and the system without any extreme. If $\lambda \geq \lambda_c$, then all fixed points are stable. If $\lambda < \lambda_c$, those fixed points which remain between two extrema are unstable.

A diagram similar to Fig. 5 can be obtained for defining stable and unstable zones of a forced system.

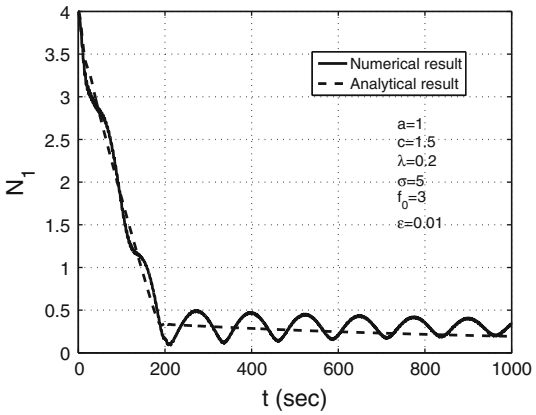

Fig. 14 Numerical and analytical results for N_1 during the forced vibration

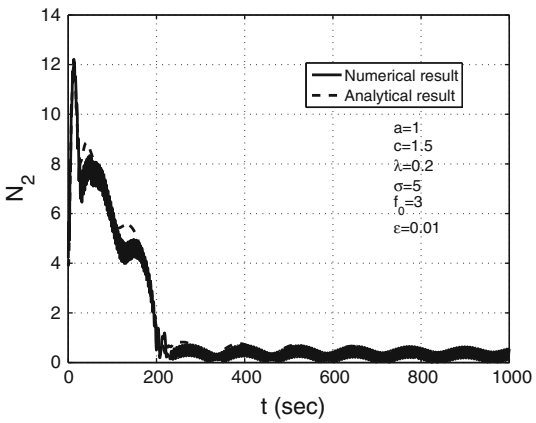

Fig. 15 Numerical and analytical results for N_2 during the forced vibration

4.4 Numerical verification

Let us define N_1 and N_2 in terms of the original system of equations:

$$N_1^{\text{exact}} = \sqrt{\omega^2(y_1 + \epsilon y_2)^2 + (\dot{y}_1 + \epsilon \dot{y}_2)^2}, \tag{67}$$

$$N_1^{\text{exact}} = \sqrt{\omega^2(y_1 - y_2)^2 + (\dot{y}_1 - \dot{y}_2)^2}. \tag{68}$$

The behavior of the system in terms of N_1 and N_2 versus time with the initial conditions (40) is illustrated in Figs. 14 and 15, respectively. Figure 15 shows that amplitude of the non-smooth NES suddenly jumps after a while and reduces abruptly. In fact, when the system reaches the vicinity of the unstable zone, it jumps to the other stable zone. After this abrupt jump of the system, numerical and analytical results do not match well but the energy of the master structure has been transferred.

As a second example, let us consider the described initial conditions in (41). The behavior of the system and the abrupt reduction of the energy of the master structure is depicted in Fig. 16 (analytical results are evaluated by endowing Eq. (17)) while Fig. 17 summarizes displacement histories of the main structure and the NES during the transient and steady-state regimes. Figure 17a shows that the displacement of the main structure reduces rapidly during the transient regime.

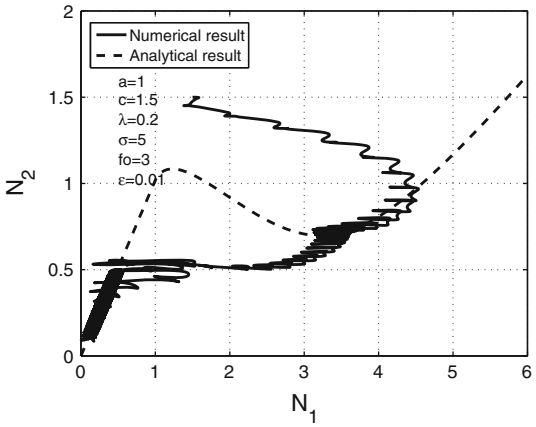

Fig. 16 Numerical and analytical results for N_1-N_2 during the forced vibration

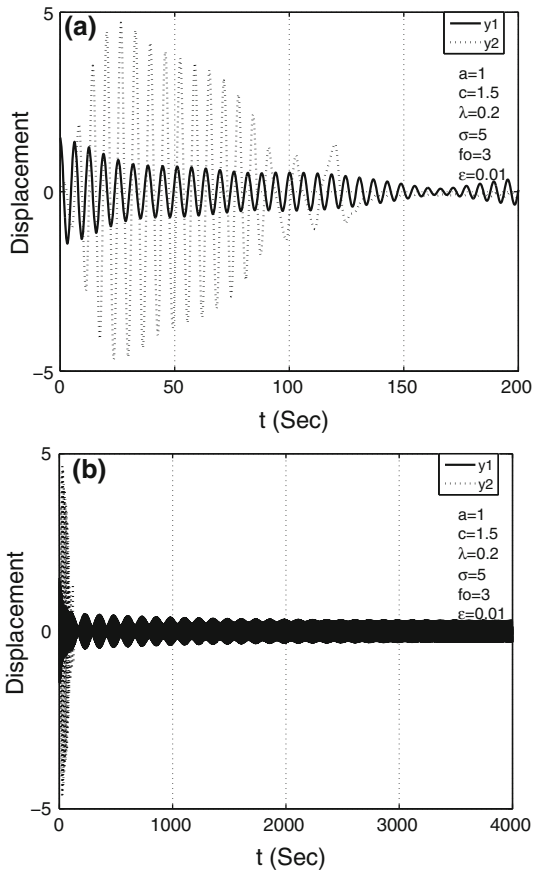

Fig. 17 Displacement histories of two oscillators during the forced vibration during: **a** transient regime; **b** steady-state regime

5 SMR response of the system

Quasi-periodic response of a linear oscillator attached to "cubic" NES under external sinusoidal forcing in the vicinity of main resonance has already studied analytically and numerically [6,29], while Starosvetsky and Gendelman [30] did a detailed investigation on the SMR of a linear system which was coupled to a cubic NES. The SMR is not related to the fixed points of average modulation equations of the system and it appears in the system as a result of global fold bifurcation of limit cycles. Here, we are interested to grasp the behavior of the non-smooth system during its SMR regime.

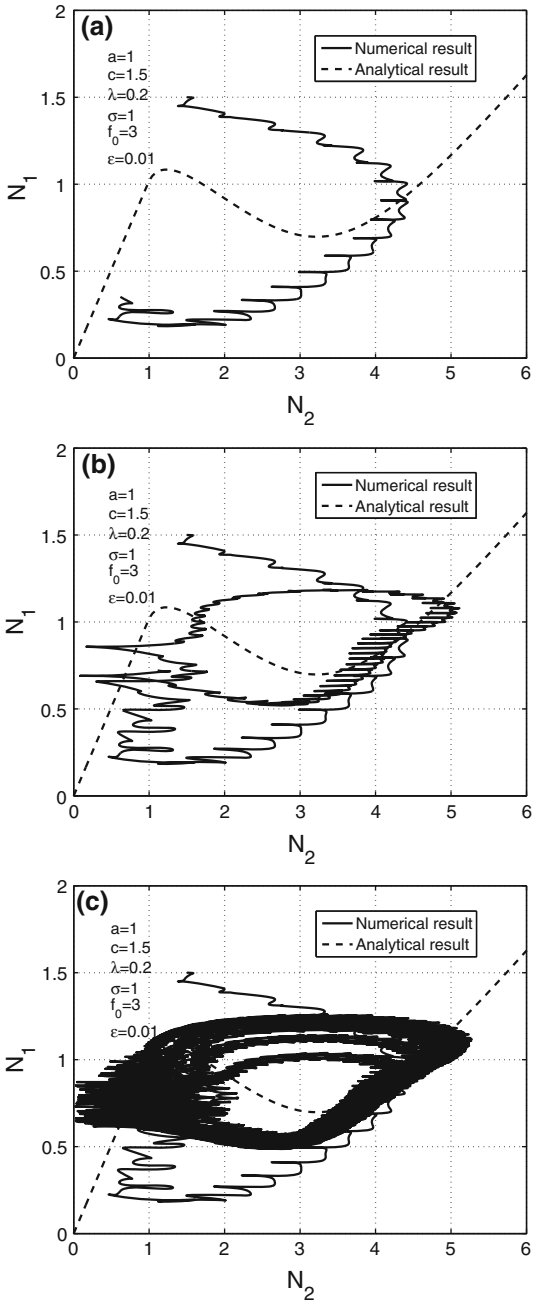

Fig. 18 Analytical and corresponding numerical results for the system until time **a** $t = 70$ s; **b** $t = 250$ s; **c** $t = 8{,}000$ s

Suppose that $\epsilon = 0.01$ and $\sigma = 1$, so $\omega = 1.01$ which is very close to the frequency of the main structure. Figures 18 summarizes obtained analytical results and corresponding numerical ones until three different times, namely $t = 70$ s, $t = 250$ s, and $t = 8{,}000$ s, for a system possessing only one unstable fixed point. These results show that the system jumps from a higher stable branch to lower one and vice versa.

If we consider the behavior of the system in some far time intervals such as $t \in [40000, 41000]$, we observe that the oscillations exhibit beating phenomenon which represents a SMR (see Fig. 19).

The same simulations are carried out for the system with $\epsilon = 0.0001$ and obtained results during the interval $t \in [40000, 95000]$ are depicted in Fig. 20 showing the hysteresis jumps between two stable branches of the system during beating phenomenon as is illustrated in Fig. 21. The Poincaré sections of the main system

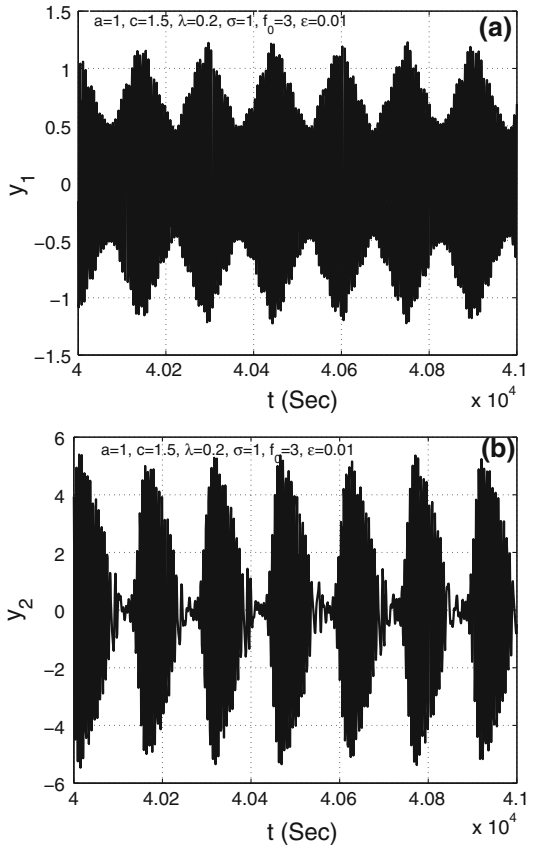

Fig. 19 Beating response of two oscillators **a** master system; **b** non-smooth NES

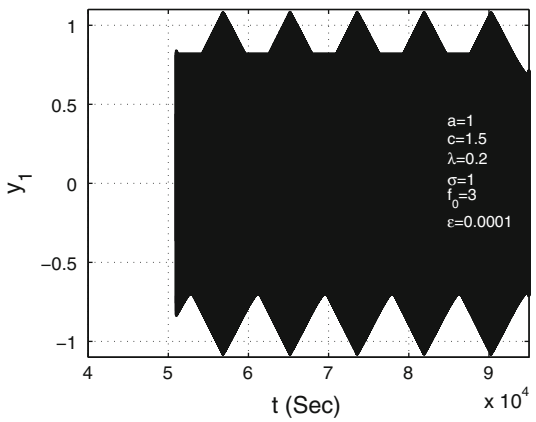

Fig. 20 Beating of the master oscillator of a system with $\epsilon = 0.0001$

and the non-smooth NES are shown in Fig. 22; both sections are closed loop sections, characterizing the strong quasi-periodic behavior of the system during forced oscillation.

5.1 Detailed investigation on the SMR of the compound non-smooth system

Let us consider the case $f_0 = 0$ and $\sigma = 0$. Figure 23 summarizes obtained numerical and analytical results for N_1 and N_2 of the system under considerations, while the phase portrait of systems (52) and (53) is shown

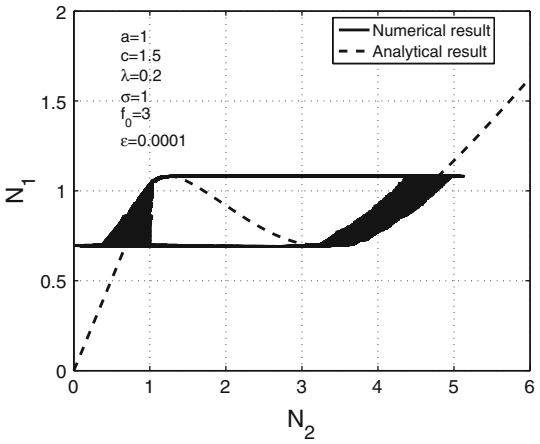

Fig. 21 Hysteresis jumps of the system during its steady-state regime in $t \in [40000, 95000]$

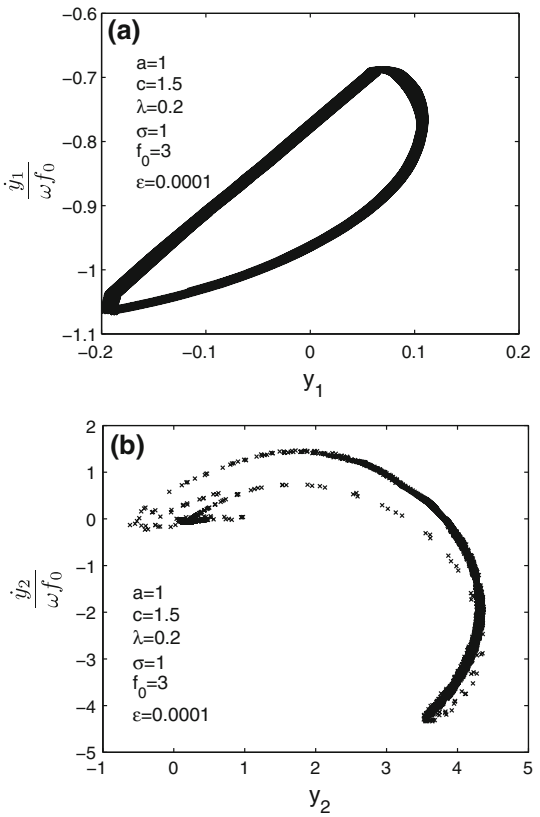

Fig. 22 Poincaré section of the **a** main oscillator; **b** non-smooth NES

in Fig. 24 by tick lines. The averaged system (46) is solved numerically for following initial conditions: $\varphi_1(0) = \varphi_2(0) = 1.2$. These results are shown by the tick continuous line in Fig. 24 as well. In this figure, the upper area of the fold line N_{22} corresponds to the upper stable branch and the lower area of the the fold line N_{21} corresponds to the lower stable branch while the bounded area between N_{22} and N_{21} in Fig. 24 represents unstable branches of the Fig. 23. With the above-mentioned initial conditions, the initial energy is greater than the upper fold line, so the system after stabilizing itself flows immediately to the upper stable branch, then reduces its amplitude and phase continuously until it experiences an abrupt jump to the lower stable branch, and afterward its amplitude goes to zero. It can be seen that all stream lines at the upper stable branch aim at the fold line N_{22}, while they aim at the zero point at the lower stable area. This means that the flow can jump

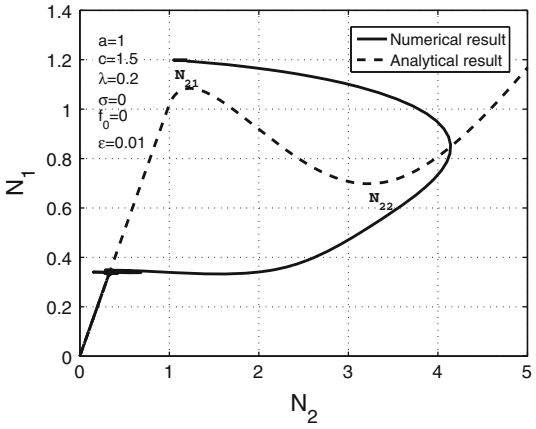

Fig. 23 Analytical and corresponding numerical results for the system under free oscillation

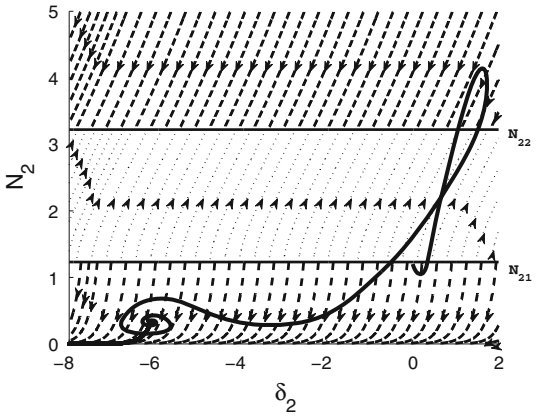

Fig. 24 Phase portrait for the system under free oscillation ($a = 1, c = 1.5, \lambda = 0.2, \sigma = 0, f_0 = 0, \epsilon = 0.01$)

from the upper stable zone to the lower stable one, while the reverse process or relaxation phenomenon for the system under free oscillation is impossible.

5.2 Necessary condition for relaxation

The possible relaxation of the system can occur if the flow in the vicinity of the lower fold line undergoes some bifurcations; this means that for some points at the lower fold, N_2' should change its sign, so phase trajectories of the lower branch can change their direction and converge toward the fold line N_{21} for a jump to the upper branch. This criterion will be satisfied if in Eqs. (52) and (53)

$$\begin{aligned} f_1(N_2, \delta_2) &= 0, \\ f_2(N_2, \delta_2) &= 0, \end{aligned} \tag{69}$$

which is equivalent to the following system:

$$\begin{bmatrix} \alpha_{11} & \alpha_{12} \\ \alpha_{21} & \alpha_{22} \end{bmatrix} \begin{bmatrix} \cos(\delta_2) \\ \sin(\delta_2) \end{bmatrix} = \begin{bmatrix} \beta_1 \\ \beta_2 \end{bmatrix}, \tag{70}$$

where

$$\begin{cases} \alpha_{11} = \lambda f_0, \\ \alpha_{12} = -f_0\left(1 - G\left(N_2^2\right)\right), \\ \alpha_{21} = -\frac{f_0\left(1-G\left(N_2^2\right)-2N_2^2G'\left(N_2^2\right)\right)}{N_2}, \\ \alpha_{22} = -\frac{\lambda f_0}{N_2}, \\ \beta_1 = \lambda N_2, \\ \beta_2 = \lambda^2(1+2\sigma) - \left(1 - G\left(N_2^2\right) - 2N_2^2G'\left(N_2^2\right)\right)\left(-2\sigma + 2\sigma G\left(N_2^2\right) + G\left(N_2^2\right)\right). \end{cases} \tag{71}$$

The system (70) has two kinds of solutions. The first kind exists when the determinant of the α-matrix is not zero, i.e. $\alpha_{11}\alpha_{22} - \alpha_{12}\alpha_{21} = -\frac{2f_0^2}{N_2^2}g(N_2) \neq 0$. Since $g(N_2) \neq 0$, these kinds of solutions correspond to the ordinary fixed points. The second kind of solutions is related to the case when the determinant of the α-matrix is zero. This corresponds to $g(N_2) = 0$; here, the singularity and equilibrium points coincide, so $N_2 = N_{21}$ or $N_2 = N_{22}$. This kind of singularities is called fold singularities. Let us consider the first equation of the system (70) when the system has folded singularities:

$$\lambda f_0 \cos(\delta_{2k}) + f_0\left(1 - G\left(N_{2k}^2\right)\right)\sin(\delta_{2k}) = \lambda N_{2k}, \tag{72}$$

or

$$\begin{aligned} &\frac{\lambda}{\sqrt{\lambda^2 + \left(1 - G\left(N_{2k}^2\right)\right)^2}}\cos(\delta_{2k}) - \frac{1 - G\left(N_{2k}^2\right)}{\sqrt{\lambda^2 + \left(1 - G\left(N_{2k}^2\right)\right)^2}}\sin(\delta_{2k}) \\ &= \frac{\lambda N_{2k}}{f_0\sqrt{\lambda^2 + \left(1 - G\left(N_{2k}^2\right)\right)^2}}, \end{aligned} \tag{73}$$

where $k = 1, 2$. We introduce a new variable γ_{0k} so that

$$\cos(\gamma_{0k}) = \frac{\lambda}{\sqrt{\lambda^2 + \left(1 - G\left(N_{2k}^2\right)\right)^2}}, \tag{74}$$

so Eq. (73) yields the following system:

$$\cos(\gamma_{0k} - \delta_{2k}) = \frac{\lambda N_{2k}}{f_0\sqrt{\lambda^2 + \left(1 - G\left(N_{2k}^2\right)\right)^2}}, \tag{75}$$

and then

$$\delta_{2k} = \gamma_{0k} \pm \arccos\left(\frac{\lambda N_{2k}}{f_0\sqrt{\lambda^2 + \left(1 - G\left(N_{2k}^2\right)\right)^2}}\right). \tag{76}$$

The first pair of folded singularities on the first fold, i.e., (N_{21}, δ_{21}) and (N_{21}, δ_{22}) exists if

$$f_0 \geq f_{0(1\text{critical})} = \frac{\lambda N_{21}}{\sqrt{\lambda^2 + \left(1 - G\left(N_{21}^2\right)\right)^2}}, \tag{77}$$

and the second pair of folded singularities on the second fold, i.e., (N_{22}, δ_{21}) and (N_{22}, δ_{22}) exists if

$$f_0 \geq f_{0(2\text{critical})} = \frac{\lambda N_{22}}{\sqrt{\lambda^2 + \left(1 - G\left(N_{21}^2\right)\right)^2}}. \tag{78}$$

According to the above-mentioned criteria, we can distinguish three different cases as follows:
$f_0 < f_{0(1\text{critical})}$:

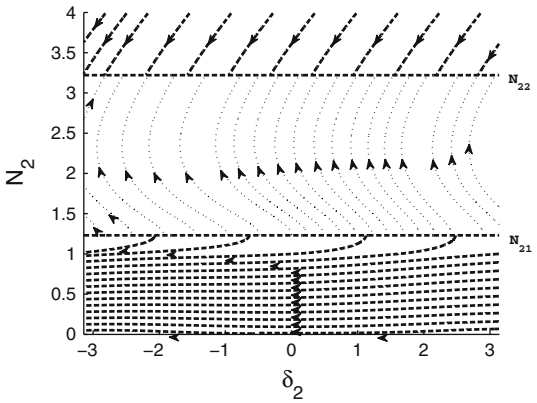

Fig. 25 Phase portrait for the system under relatively low external forcing term $f_0 = 0.1 < f_{0(1critical)} = 0.279$ ($a = 1$, $c = 1.5, \lambda = 0.2, \sigma = 2, \epsilon = 0.01$)

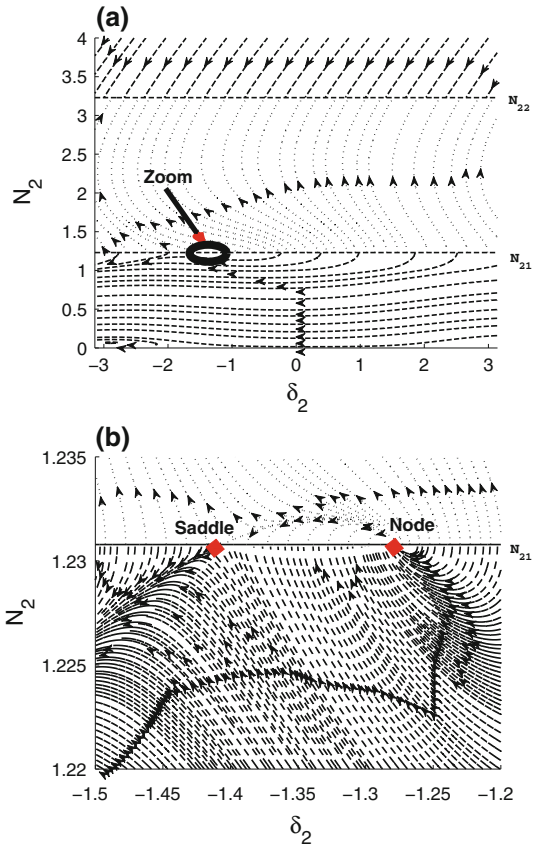

Fig. 26 Phase portrait for the system under forcing term $f_{0(1\text{critical})} = 0.279 < f_0 = 0.28 < f_{0(2critical)} = 2.97$ ($a = 1$, $c = 1.5, \lambda = 0.2, \sigma = 2, \epsilon = 0.01$), **a** the overall view; **b** the zoomed area

This is the case when external forcing is relatively small; there is not any bifurcation nor folded singularities near the fold line N_{21}. The relaxation is impossible. Figure 25 illustrates the behavior of the system when $f_0 = 0.1 < f_{0(1\text{critical})} = 0.279$. In the lower stable zone and in the vicinity of the fold line N_{21}, none of the streams change their directions and consequently there is no folded singularity.

$f_{0(1\text{critical})} \leq f_0 < f_{0(2\text{critical})}$:

When $f_0 = f_{0(1\text{critical})}$, then saddle and node coincide and they can be evaluated just by γ_{0k} in Eq. (76). By increasing the force, folded singularities gradually become distinct and near the fold line directions of streams change and between two folded singularities streams converge toward the fold line N_{21}. Figure 26a depicts

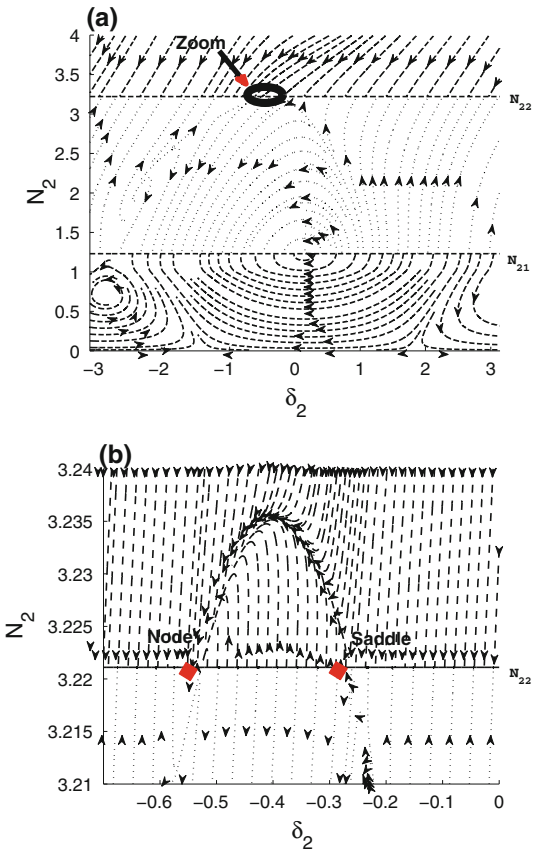

Fig. 27 Phase portrait for the system under under external forcing term $f_0 = 3 > f_{0(2critical)} = 2.97$ ($a = 1, c = 1.5$, $\lambda = 0.2, \sigma = 2, \epsilon = 0.01$), **a** the overall view; **b** the zoomed area

the case when folded singularities of a system with external forcing $f_0 = 0.28 > f_{0(1\text{critical})} = 0.279$ start to become distinct. The detail is illustrated in Fig. 26b. The saddle and node singularities of the system are $\delta_{21-\text{Saddle}} = -1.41$ and $\delta_{21-\text{Node}} = -1.28$, respectively. The latter figure shows that streams between folded singularities change their directions and aim at the fold line N_{21} which gives a hint of existence of the possible relaxation.

$f_0 \geq f_{0(2\text{critical})}$:

In this case, folded singularities fell on the fold line N_{22}. Let us consider the system with a forcing term $f_0 = 3$ ($f_{0(2\text{critical})} = 2.97$). Behavior of the system is illustrated in Fig. 27a showing that folded singularities are on the fold line N_{21}. Zoomed area of the Fig. 27a is depicted in Fig. 27b and it can been seen that the saddle and node singularities of the system are $\delta_{22-\text{Saddle}} = -0.26$ and $\delta_{22-\text{Node}} = -0.53$, respectively.

The condition $f_0 > f_{0(1\text{critical})}$ is a necessary condition for the system in order to face a SMR, but it is not sufficient. Initial condition of the system and σ parameter lead the system to three different behavior as it follows:

- permanent SMR;
- permanent periodic after a transient relaxation oscillation;
- permanent periodic regime.

Figure 28 summarizes the behavior of a system for fixed parameters but varying σ, namely $\sigma = 1, 2, 3$. As it can be seen in Fig. 28a when $\sigma = 1$, there is no fixed point in the system and the only stable regime is SMR. By increasing the value of the σ, the fixed points of the system remain at the lower stable part and the system can face relaxation then experiences the periodic regime (Fig. 28b) or it experiences just the periodic regime without any relaxation (Fig. 28c). The fixed point of the system can be located at the upper stable zone

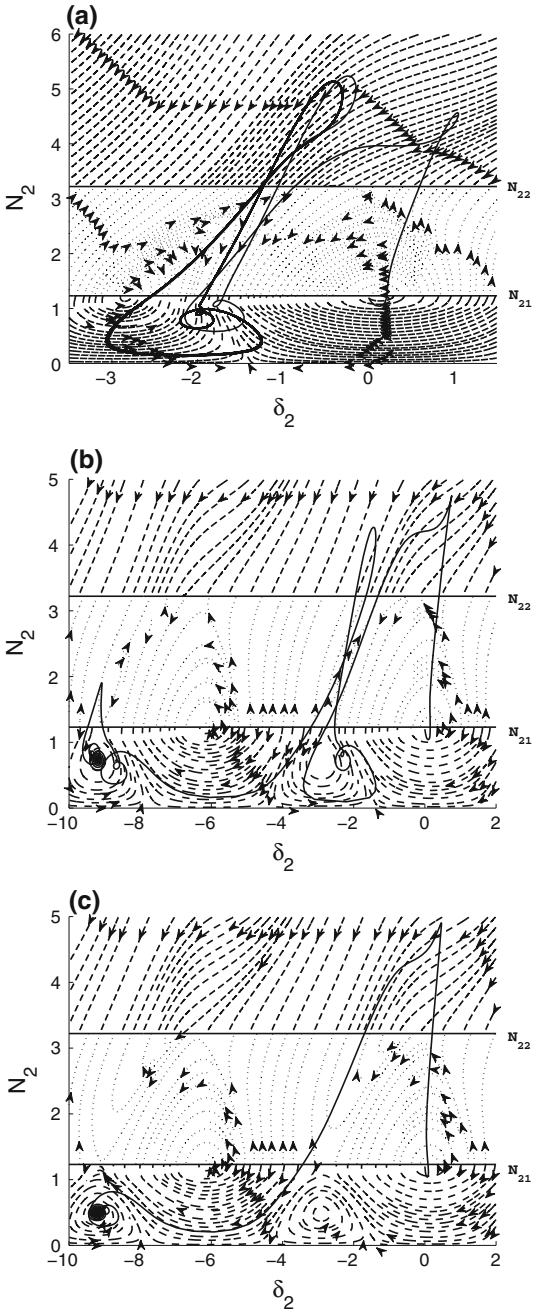

Fig. 28 Phase portrait for the system under external forcing term $f_0 = 3 > f_{0(2\text{critical})} = 2.97$ ($a = 1, c = 1.5, \lambda = 0.2$, $\epsilon = 0.01$, $N_2(0) = 1.2$), **a** $\sigma = 1$; **b** $\sigma = 2$ **c** $\sigma = 3$

for very large external forces. This case is not interesting from the TET view point and it should be avoided (see Fig. 29).

6 Conclusion

A 2 dof system with a nonlinear energy sink device under impulse and sinusoidal loadings is studied analytically and numerically. The nonlinearity of the energy sink is replaced by a non-smooth piece-wise linear function for the sake of practical investigations. It is seen that the main system is able to transfer the majority

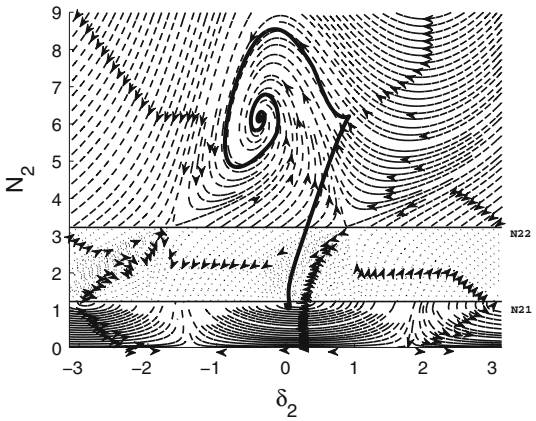

Fig. 29 Phase portrait for the system under external forcing term $f_0 = 10 > f_{0(2\text{critical})} = 2.97$ ($a = 1, c = 1.5, \lambda = 0.2$, $\sigma = 1, \epsilon = 0.01, N_2(0) = 1.2$), **a** $\sigma = 1$; **b** $\sigma = 2$ **c** $\sigma = 3$

of its energy during a 1:1 resonance to the non-smooth device by an abrupt jump from the upper stable system branch to its lower stable branch; moreover, the system under forcing and during its 1:1 resonance can lead to a strongly modulated response which is characterized by a relaxation phenomenon between stable branches of the system.

Acknowledgments This work has been supported by "Agence Nationale de la Recherche" (ANR) in the frame of the project ADYNO ANR-07-BLAN-0193.

References

1. Vakakis, A.F.: Inducing passive nonlinear energy sinks in vibrating systems. ASME J. Vib. Acoust. **123**, 324–332 (2001)
2. Gendelman, O.V., Manevitch, L.I., Vakakis, A.F., M'Closkey, R.: Energy pumping in nonlinear mechanical oscillators I: dynamics of the underlying Hamiltonian systems. ASME J. Appl. Mech. **68**, 34–41 (2001)
3. Vakakis, A.F., Gendelman, O.V.: Energy pumping in nonlinear mechanical oscillators II: resonance capture. ASME J. Appl. Mech. **68**, 42–48 (2001)
4. Gendelman, O.V.: Bifurcations of nonlinear normal modes of linear oscillator with strongly nonlinear damped attachment. Nonlinear Dyn. **37**, 115–128 (2004)
5. Gendelman, O.V., Lamarque, C.-H.: Dynamics of linear oscillator coupled to strongly nonlinear attachment with multiple states of equilibrium. Chaos, Solitons Fractals **24**, 501–509 (2005)
6. Gendelman, O.V., Gourdon, E., Lamarque, C.-H.: Quasiperiodic energy pumping in coupled oscillators under periodic forcing. J. Sound Vib. **294**, 651–662 (2006)
7. Manevitch, L.I., Gourdon, E., Lamarque, C.-H.: Parameters optimization for energy pumping in strongly nonhomogeneous 2 DoF system. Chaos Solitons Fractals **31**, 900–911 (2007)
8. Manevitch, L.I., Musienko, A.I., Lamarque, C.-H.: New analytical approach to energy pumping problem in strongly non homogeneous 2 DoF systems. Meccanica **42**, 77–83 (2007)
9. Manevitch, L.I., Gourdon, E., Lamarque, C.-H.: Towards the design of an optimal energetic sink in a strongly inhomogeneous two-degree-of-freedom system. Trans. ASME **2007**(74), 1078–1086 (2007)
10. Vakakis, A.F., Gendelman, O.V., Bergman, L.A., McFarland, D.M., Kerschen, G., Lee, Y.S.: Nonlinear Trageted Energy Transfer in Mechanical and Structural Systems I, 375. Springer, Berlin (2009)
11. Vakakis, A.F., Gendelman, O.V., Bergman, L.A., McFarland, D.M., Kerschen, G., Lee, Y.S.: Nonlinear Trageted Energy Transfer in Mechanical and Structural Systems II, 655. Springer, Berlin (2009)
12. Starosvetsky, Y., Gendelman, O.V.: Vibration absorption in systems with nonlinear energy sink: nonlinear damping. J. Sound Vib. **324**, 916–939 (2009)
13. Starosvetsky, Y., Gendelman, O.V.: Interaction of nonlinear energy sink with a two degrees of freedom linear system: internal resonance. J. Sound Vib. **329**, 1836–1852 (2010)
14. Gendelman, O.V., Sapsis, T., Vakakis, A.F., Bergman, L.A.: Enhanced passive targeted energy transfer in strongly nonlinear mechanical oscillators. J. Sound Vib., Rapid Communication, **330**, 1–8 (2011)
15. McFarland, D.M., Bergman, L., Vakakis, A.F.: Experimental study of non-linear energy pumping occurring at a single fast frequency. Int. J. Non-Linear Mech. **40**, 891–899 (2005)
16. McFarland, D.M., Kerschen, G., Kowtko, J.J., Lee, Y.S., Bergman, L.A., Vakakis, A.F.: Experimental investigation of targeted energy transfers in strongly and nonlinearly coupled oscillators. J. Acoust. Soc. Am. **118**, 791–799 (2005)
17. Kerschen, G., Kowtko, J.J., McFarland, D.M., Bergman, L.A., Vakakis, A.F.: Theoretical and experimental study of multimodal targeted energy transfer in a system of coupled oscillators. Nonlinear Dyn. **47**, 285–309 (2007)

18. Kerschen, G., Kowtko, J.J., McFarland, D.M., Lee, Y.S., Bergman, L.A., Vakakis, A.F.: Experimental demonstration of transient resonance capture in a system of two coupled oscillators with essential stiffness nonlinearity. J. Sound Vib. **299**, 822–838 (2007)
19. Gourdon, E., Alexander, N.A., Taylor, C.A., Lamarque, C.-H., Pernot, S.: Nonlinear energy pumping under transient forcing with strongly nonlinear coupling: theoretical and experimental results. J. Sound Vib. **300**, 522–551 (2007)
20. Gourdon, E., Lamarque, C.-H., Pernot, S.: Contribution to efficiency of irreversible passive energy pumping with a strong nonlinear attachment. Nonlinear Dyn. **50**, 793–808 (2007)
21. Lee, Y.S., Kerschen, G., McFarland, D.M., Hill, W.J., Nichkawde, C., Strganac, T.W., Bergman, L.A., Vakakis, A.F.: Suppressing aeroelastic instability using broadband passive targeted energy transfers, part 2: experiments. AIAA J. **45**, 2391–2400 (2007)
22. Lee, Y.S., Vakakis, A.F., Bergman, L.A., McFarland, D.M., Kerschen, G., Nucera, F., Tsakirtzis, S., Panagopoulos, P.N.: Passive non-linear targeted energy transfer and its applications to vibration absorption: a review. In: Proceedings of the institution of mechanical engineers, Part K. J. Multi-body Dyn. **222**, 77–134 (2008)
23. Lee, Y.S., Vakakis, A.F., McFarland, D.M., Bergman, L.A.: Non-linear system identification of the dynamics of aeroelastic instability suppression based on targeted energy transfers. Aeronaut. J. **114**, 61–82 (2010)
24. Nucera, F., Vakakis, A.F., McFarland, D.M., Bergman, L.A., Kerschen, G.: Targeted energy transfers in vibro-impact oscillators for seismic mitigation. Nonlinear Dyn. **50**, 651–677 (2007)
25. Lee, Y.S., Nucera, F., Vakakis, A.F., McFarland, D.M., Bergman, L.A.: Periodic orbits, damped transitions and targeted energy transfers in oscillators with vibro-impact attachments. Phys. D **238**, 1868–1896 (2009)
26. Gendelman, O.V.: Targeted energy transfer in systems with non-polynomial nonlinearity. J. Sound Vib. **315**, 732–745 (2008)
27. Manevitch, L.I.: The description of localized normal modes in a chain of nonlinear coupled oscillators using complex variables. Nonlinear Dyn. **25**, 95–109 (2001)
28. Nayfeh, A.H., Mook, D.T.: Nonlinear Oscillations, 720. Wiley, New York (1979)
29. Gendelman, O.V., Starosvetsky, Y.: Quasi-periodic response regimes of linear oscillator coupled to nonlinear energy sink under periodic forcing. J. Appl. Mech. **74**, 325–331 (2007)
30. Starosvetsky, Y., Gendelman, O.V.: Strongly modulated response in forced 2DOF oscillatory system with essential mass and potential asymmetry. Phys. D **237**, 1719–1733 (2008)